Post-Laramide, Eocene magmatic activity in Sierra de Catorce, San Luis Potosí, México

Eduardo Mascuñano[1], Gilles Levresse[1,*], Esteve Cardellach[2], Jordi Tritlla[1], Rodolfo Corona-Esquivel[3], and Christine Meyzen[4]

[1] Geofluidos, Centro de Geociencias, Universidad Nacional Autónoma de México, Blvd. Juriquilla No. 3001, 76230 Querétaro, Mexico.
[2] Departament de Geologia de la Universitat Autònoma de Barcelona, Edifici Cs, 08193-Cerdanyola del Vallès, Spain.
[3] Instituto de Geología, Universidad Nacional Autónoma de México, Ciudad Universitaria, 04510 México, D.F., Mexico.
[4] Dipartimento di Geoscienze, Università degli Studi di Padova, Via G. Gradenigo, 35131 Padova, Italia.
**glevresse@geociencias.unam.mx*

ABSTRACT

The Sierra de Catorce is a N-S-trending mountain range located in the northeastern portion of the Mesa Central physiographic province, Mexico. The Sierra lies at the northern end of the Taxco-San Miguel de Allende fault system, which is interpreted as the surface expression of a major crustal discontinuity. A Triassic to upper Cretaceous sedimentary succession, deformed during the Laramide orogeny, crops out in the range. From the structural point of view, the Sierra de Catorce is a double plunging anticlinorium bounded in its western side by a post-Laramide N-S-trending and west dipping normal fault. We report geochronologic and geochemical data for several post-tectonic granitoids cropping out in the range. The intrusive bodies are I-type continental arc granitoids with Eocene instrusion ages (ca. 38 to 45 Ma, U-Pb determined by LA-ICPMS on individual zircon crystals). Epithermal argentiferous ore deposits are spatially associated with the granitoids. The geochemical signature of the granitoids indicates that magmas derived from a metasomatized mantle, and were highly contaminated with crustal materials. Despite the inferred position of the subduction zone during the Eocene (over 600 km westward), an influence of the subducted slab is needed to explain the metasomatization of the mantle wedge and the high-Ba content observed in all the Sierra de Catorce granitoids. Geochemical features of the granitic rocks are consistent with the regional and local geological framework that allowed rapid emplacement of magma pulses in a post-orogenic extensional geodynamic setting.

Key words: post-orogenic magmatism, petrogenesis, U-Pb dating, granitoids, Eocene, Sierra de Catorce, Mexico.

RESUMEN

La Sierra de Catorce se ubica en el límite nororiental de la provincia fisiográfica de la Mesa Central. La sierra está constituida principalmente por formaciones sedimentarias de edad mesozoica, las cuales están plegadas formando un doble anticlinal orientado N-S y recumbente hacia el E, formado durante la deformación laramídica. El límite occidental es una falla normal que forma parte del sistema

Mascuñano, E., Levresse, G., Cardellach, E., Tritlla, J., Corona-Esquivel, R., Meyzen, C., 2013, Post-Laramide, Eocene magmatic activity in Sierra de Catorce, San Luis Potosí, México: Revista Mexicana de Ciencias Geológicas, v. 30, núm. 2, p. 299-311.

Taxco - San Miguel de Allende, el cual se considera la expresión superficial de una discontinuidad de la corteza continental de México. Varias intrusiones magmáticas se emplazaron durante eventos extensivos posorogénicos. Los cuerpos intrusivos están relacionados espacialmente con depósitos argentíferos epitermales encajados en calizas mesozoicas. Las edades isotópicas de los intrusivos graníticos varían entre 38 y 45 Ma (U-Pb en circones, LA-ICPMS). La firma geoquímica de estos granitoides es de arco continental de tipo I, formados a partir de un magma derivado del manto metasomatizado, altamente contaminado por materiales corticales. A pesar de la posición de la zona de subducción durante el Eoceno (más de 600 km hacia el W), es preciso recurrir a una subducción plana de más de 600 km para explicar tanto la metasomatización del manto como el alto contenido de Ba observado en todas las muestras. Las características geoquímicas de los granitoides son coherentes con la geología regional y local, la cual controló el emplazamiento rápido de pulsos de magmas relacionados con el ambiente geodinámico extensional poscolisión.

Palabras clave: magmatismo posorogénico, petrogénesis, fechamiento U-Pb, granitoides, Eoceno, Sierra de Catorce, México.

INTRODUCTION

The Sierra de Catorce range (SDCR) is an important historic mining region located in central Mexico (Figure 1). The region is divided into four metallogenetic districts; three of them are magmatic-related: (1) the historical Real de Catorce (Ag-Au-Pb-Zn), (2) La Paz Cu-Au skarn and associated Ag-Pb-Zn veins (Pinto-Linares *et al.*, 2008), and (3) La Maroma prospect, where evidence exists for Au-Ag-Pb mineralization (Chippendale, 1910). The Wadley simple-Sb and stratabound deposits constitute the fourth district in the range (White and Gonzáles, 1946; Zárate del Valle, 1982). Despite its historical mining importance, the SDCR has received little attention from geoscientists. In the last thirty years, just a few studies on the geological environment of the different deposits have been published (*e.g.*, Carrizales-Ibarra, 1989; Gunnesch *et al.*, 1994; Pinto-Linares *et al.*, 2008). Regional geological studies have been focused on the characterization of the Mesozoic stratigraphic sequence (*e.g.*, Carrillo-Bravo, 1968; Blauser, 1979; Geoffrey, 1979; Barboza-Gudiño *et al.*, 1998, 2004, 2008; Olóriz *et al.*, 1999; Hoppe, 2000; Martínez-Macías, 2004).

The characterization of the different intrusive bodies and other minor extrusive materials is almost limited to K-Ar dating (whole rock, 53 ± 4 Ma, Real de Catorce, Mújica-Mondragón and Jacobo-Albarrán, 1983; *ca.* 35.7 ± 1.0 Ma in biotite, Fraile, Tuta *et al.*, 1988). Only the Fraile Cu-Au skarn and Ag-Pb-Zn associated veins have received more attention in this sense, including U-Pb dating and geochemical studies (Pinto-Linares *el al*., 2008).

In this study, we present new geochemical data for granitoids and basaltic rocks of the SDCR to elucidate the possible magma sources, and U-Pb zircon data for some samples of felsic granitoids.

GEOLOGICAL SETTING

The SDCR is located in the eastern border of the Mesa Central, in central Mexico. The Mesa Central is an elevated plateau partly covered by Cenozoic volcanic sequences, affected by the Eocene and Oligocene east-west extension (Nieto-Samaniego *et al.*, 2005) that created a series of deep continental basins, which are now partially filled with alluvial and lacustrine sediments. The eastern tectonic boundary of the Mesa Central is the Taxco-San Miguel de Allende fault system, a regional structure that extends across the Trans-Mexican Volcanic Belt, in a N-S direction, from the Taxco mining district in southern Mexico to the SDCR region (Demant, 1978, Alaniz-Álvarez and Nieto-Samaniego, 2005).

The oldest rocks exposed in the Mesa Central are Triassic marine turbidites, which are overlain, along the Mesa Central, by Lower and Middle Jurassic continental rocks, including volcanic flows, conglomerates and sandstones, and an Upper Jurassic to Upper Cretaceous marine sedimentary succession (Barboza-Gudiño *et al.*, 2012). Cenozoic materials are mostly represented by continental conglomerates and volcanic rocks of andesitic to rhyolitic composition. The last Cenozoic magmatic felsic event is characterized by the presence of F-rich topaz rhyolites (Orozco-Esquivel *et al.*, 2002). Locally, mafic alkalic lava flows and associated pyroclastics of Miocene to Quaternary age are also exposed (Aranda-Gómez and Luhr, 1996; Luhr and Aranda-Gómez, 1997). The Laramide orogeny affected the entire Mesozoic sedimentary column causing folding and reverse faulting in the whole Mesa Central, and in the northeast corner caused the uplift of the SDCR (Barboza-Gudiño *et al.*, 2012).

The detailed stratigraphic column of the Sierra de Catorce range was fully described by Barboza-Gudiño *et al.* (1998, 2004). Briefly, the oldest outcrops are siliciclastic sediments of the Triassic Zacatecas Formation. The stratigraphic succession is continuous from Oxfordian to Maastrichtian. The Jurassic succession is represented by the volcanoclastic Nazas and La Joya formations, and by the sedimentary the Zuloaga and La Caja formations. From bottom to top, the Cretaceous succession is composed by the the Taraises, Lower Tamaulipas, Otates, Upper Tamaulipas, Cuesta del Cura, Indidura, and Caracol marine sedimentary formations.

The SDCR is a double plunging, N-S trending anti-

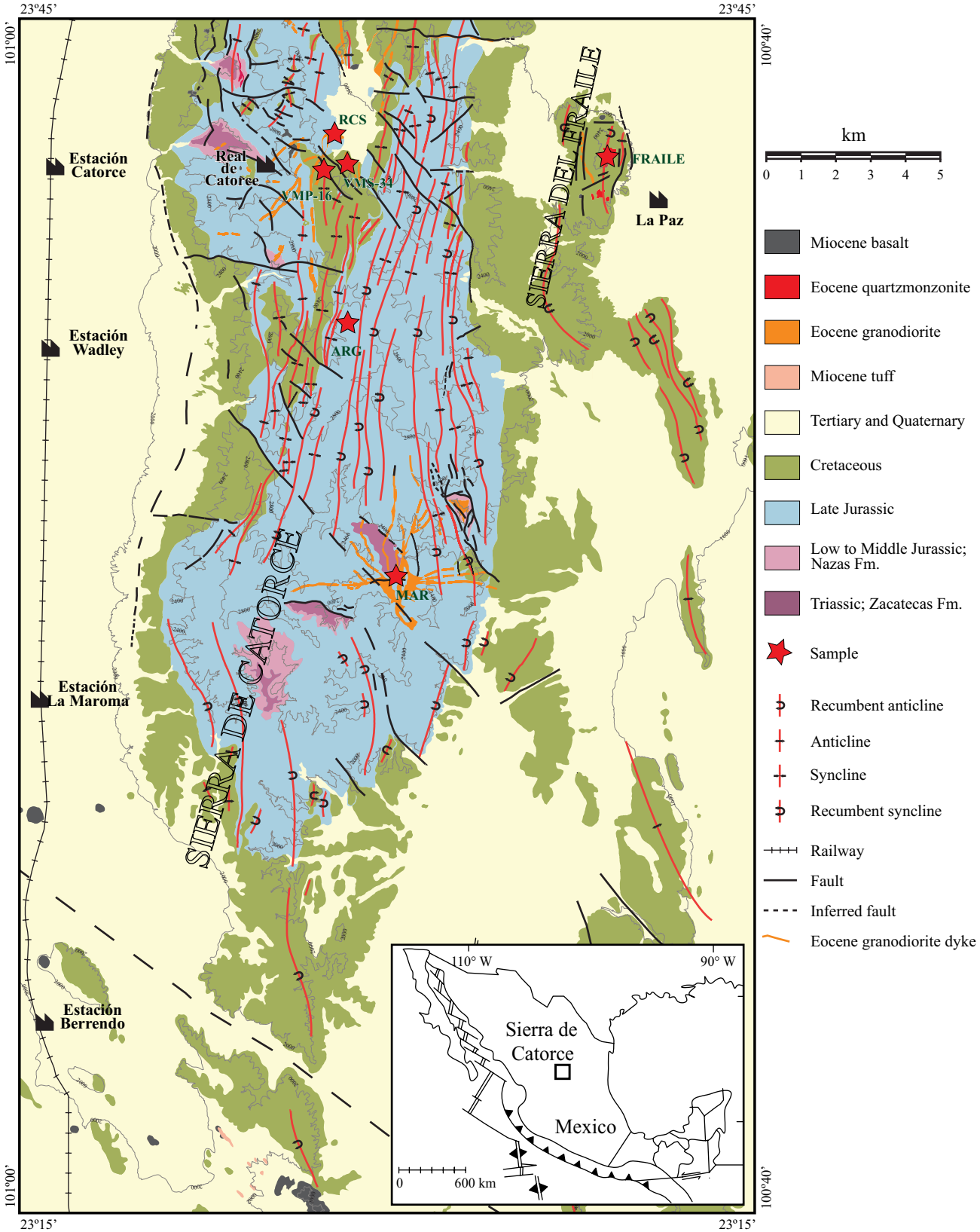

Figure 1. Geological sketch map of the Sierra de Catorce and Fraile area (modified from Barboza-Gudiño *et al.,* 1998). ARG: Los Alamitos; MAR: La Maroma; RCS: Real de Catorce; VMP-16 and VMS-34: borehole samples within the Real de Catorce Ag-mineralized area.

clinorium, recumbent to the east (Figure 1). A Pleistocene to Recent alluvial cover fills up the basins developed immediately E and W of the SDCR. One of the most conspicuous Cenozoic structures in the region is a N-S-trending, west dipping normal fault, which constitutes the western limit of the SDCR. This fault crosscuts a NW-SE strike-slip fault system, which appears to be related to a Neogene reactivation of a segment of the Taxco San Miguel de Allende fault system (TSMAFS; Pinto-Linares *et al.*, 2008). This fault system is more obvious in the central part of the range, than at its north and south tips (Figure 1). White and Gonzáles (1946) assumed that the NW-SE strike-slip faults systems observed in the SDCR formed locally during the early Paleogene Laramide compression that produced the anticlinorium and associated thrust faults. All the fault systems in the SDCR present evidence of complex polyphase movements. The Sierra del Fraile is a minor range (5.5 km length), located northeast of the northern tip of SDCR and is part of the same SDCR fold system developed during the Laramide orogeny.

In the SDCR, five post-Mesozoic intrusions are recognized. La Maroma intrusive is exposed in two outcrops in the southern part of the SDCR. The largest one is in the central part of the range and is almost 3.5 km^2 wide. The second outcrop lies about 5 km toward the northeast and is only 0.5 km^2 wide. Dikes are radiating from the main body. These granitoids crosscutt the Oxfordian Zuloaga formation (limestone), causing a partial recrystalization of the host rock at the contact. About 12 km north of the La Maroma intrusive, the Los Alamitos ranch granite (ARG) occurs. It is formed by a semicircular granitic body with a exposed surface of 200 m^2. It is also hosted by the Zuloaga formation. No metasomatism or alteration was recognized in the contact of the intrusive body with the host rock.

The Real de Catorce stock (RCS) occurs in the vicinity of the homonimous town (Figure 1). It is exposed in several granitic outcrops with almost 1 km^2 of total exposed surface. These different bodies are hosted by limestones including the Oxfordian Zuloaga Fm. to the Hauterivian Lower Tamaulipas Fm. The intrusion of these bodies caused a slight alteration and recrystallization by contact metamorphism. Mújica-Mondragón and Jacobo-Albarrán (1983) reported a K-Ar age of 53 ± 4 Ma for plagioclase separated from the RCS. These intrusive bodies are spatially connected by a network of NE-SW and N-S striking dykes. These dikes are up to 7 meters in thickness and over 2 km in length and show the same intrusive relation with the country rocks as the RCS. No major alteration was observed in the host rocks. The crosscutting relations of these dykes with the main intrusive bodies could not be established in the field.

In the nearby Sierra del Fraile, Pinto-Linares *et al.* (2008) report quartz-monzonite intrusive stocks dated by U-Pb at *ca.* 36 Ma. This body is exposed in the northern part of the Sierra del Fraile, in a 0.3 km^2 wide outcrop. A second outcrop with similar extension lies about one kilometer to the south. These stocks intruded Cenomanian and Turonian limestones of El Abra and Indiura Formation, causing intense contact metamorphism with development of an economic Cu-Au skarn deposits and Ag-Pb-Zn associated veins.

The youngest magmatic event in the region corresponds to relatively small volumes of basaltic flows, which crop out on the vicinity of Real de Catorce. These flows are arranged in minor volcanic bodies, and some gross stratification (up to 2 meters thick) can be recognized locally. The total exposed surface of these rocks is difficult to establish. They are widespread in the northern part of the SDCR forming minor outcrops 100–200 m^2 in size. The whole sedimentary column and the granitoids are crosscut by these basalts (Barboza-Gudiño *et al.*, 2004). These rocks are also observed to the west (Los Encinos, and Sierra del Fraile) and to the north (San Juan de Vanegas), where numerous volcanic necks and lava flow remnants of Miocene hawaiites were dated at 13–10 Ma ($^{40}Ar/^{39}Ar$ in plagioclase, Luhr and Aranda-Gómez, 1997).

The main objective of this study is to characterize from the geochronologic and geochemical point of view the post-Mesozoic granitoids of the Sierra de Catorce.

ANALYTICAL TECHNIQUES

Petrography. Magmatic and alteration relationships were documented through field observations, and further completed with petrographic and SEM analyses. Mineral phases were identified with a SEM-EDX at the Laboratorio de Geofluidos in the Centro de Geociencias, Universidad Nacional Autónoma de México, in Juriquilla, Querétaro (CGEO).

Zircon separation. Six rock samples from the granitic intrusive bodies were collected (Figure 1; red stars). The samples were crushed, powdered, and sieved (200 to 50 mesh). Heavy mineral fractions were obtained by density preconcentration with heavy liquids (methylene iodide). The non-magnetic fraction was separated with a Franz isodynamic magnet. Final zircon separates were hand picked under a binocular microscope and mounted in epoxy resin together with a standard (NIST), and subsequently polished. Laser ablation target points were selected on cathodoluminiscence images in order to identify zircon cores and overgrowth zones.

U-Pb age dating. The zircon samples were analyzed at the laser ablation system facility at Laboratorio de Estudios Isotópicos (LEI), Centro de Geociencias, UNAM. The instrument consists of a Resonetics excimer laser ablation workstation (Solari *et al.,* 2010), coupled with a Thermo X^{II}-Series quadrupole ICPMS. The laser ablation workstation operates a Coherent LPX 200, 193 nm excimer laser and an optical system equipped with a long working-distance lens with 50–200 μm focus depth. The ablation cell is He-pressurized capable of fast signal uptake and washout. The drill size employed during this work was of 34 μm, and the

drill depth during the analysis is about 20–25 μm, for a total mass ablated during each analysis of ~ 70–80 ng.

Seventeen isotopes are scanned during each analysis. This allows a quantitative measurement of those isotopes necessary for U-Pb dating (lead, uranium and thorium), as well as detailed monitoring of major and trace elements such as Si, P, Ti, Zr and REEs, which can yield important information on the presence of microscopic inclusions in the zircons (*e.g.* monazite, apatite, or titanite) that produce erroneous age results. For each analysis, 25 s of signal background are monitored, followed by 30 s of signal with laser firing with a frequency of 5 Hz and an energy density of ~ 8 J/cm^2 on target. The remnants 25 second are employed for washout and stage repositioning. A normal experiment involves the analysis of natural zircon standards, as well as standard glasses. NIST standard glass analyses are used to recalculate the U and Th concentration in zircon. Repeated standard measurements are in turn used for mass-bias correction, as well as for calculation of down-hole and drift fractionations.

Geochemical analysis. Major elements were determined by X-ray fluorescence spectroscopy (XRF) using a Siemens SRS-3000 instrument at the Laboratorio Universitario de Geoquímica Isotópica (LUGIS), UNAM, Mexico City. Procedures are described by Lozano and Bernal (2005).

Trace element data were obtained by inductively-coupled plasma mass spectrometry (ICP-MS) at the CGEO, using a Thermo Series X^{II} instrument, and following procedures reported by Mori *et al.* (2007).

RESULTS

Six samples of granitoids were collected from the SDCR for dating and analyses (major and trace elements; Figure 1). From south to north, the granitoid samples come from La Maroma stock (MAR), Los Alamitos ranch stock (ARG), the Real de Catorce stock (RCS), two dykes from borehole samples within the Real de Catorce Ag-mineralized area (VMP-16 and VMS-34), and a quartz monzonite from the Sierra del Fraile (Figure 1).

The Real de Catorce stock (RCS) outcrops are completely weathered, witnessed by a variety of ochre colours. Due to this intense wheathering, no fresh samples could be collected for chemical analysis. However, a sample of weathered granite (sand) was collected and processed for zircon dating.

Lithologic and petrographic description

All studied stocks and dykes from La Maroma to Real de Catorce (MAR, RCS, VMP-16 and VMS-34) are characterized by a porphyritic texture.

The Maroma granodioritic body (MAR) has porphyritic texture and shows pale ochre to greenish-gray colour in intense weathered surfaces. In less weathered surfaces, the rock presents a pale green colour mottled with white or translucid centimetric phenocrysts. In fresh surfaces, the rock is green, and centimetric phenocrysts of feldspar (up to 3 cm in size) and quartz can be easily recognized. Minor pyrite cubes (up to 2 millimetres in size) are also recognized in hand specimen.

The two borehole samples collected within the Real de Catorce Ag-mineralized area were selected from various drill cores, obtained during an exploration campaign in the Real de Catorce argentiferous mines. The samples come from the granitic veins found in the mineralized zone. The analyzed cores show a green colour mottled with phenocrysts of feldspar (up to 4 cm) and quartz (up to 0.8 cm). In thin section, phenocrysts are zoned plagioclase (21% – 40%), quartz (24% – 30%), K-feldspar (19% – 34%), mafic minerals (biotite + hornblende, 3% – 5%), and disseminated sulphides (pyrite, 3% – 5 %). Zircon, apatite, and titanite are accessory phases included in a groundmass composed of quartz and feldspar microliths (Figure 2). Phenocryst size in the dykes (VMP-16 and VMS-34) is significantly smaller than in the stocks from Real de Catorce. Quartz phenocrysts are partially resorbed; in thin section they appear rounded and with embayments. Locally, plagioclase and K-feldspar are intensely altered to sericite.

The Los Alamitos ranch stock (ARG) is brown in outcrop, showing less developed weathering. In hand specimen phenocrysts of feldspars and minor quartz are recognized. In thin section, the groundmass is formed mainly by plagioclase and K-feldespar in microcrystals up to 0.3 mm long. Quartz and orthoclase, representing up to 25% to 35% of the crystals, and are up to 1 cm in diameter and show evidence of resorption. A single crystal of microcline was identified. Some crystals of quartz and orthoclase bear plagioclase micro-inclusions 0.1 mm in size. The phenocrysts of plagioclase are up to 0.5 mm (20% of the crystals) and may show xenocrysts cores and overgrowths. Biotite altered to argillaceous minerals (5% – 10%), and apatite in partially resorbed, elongated microxenocrysts (<0.3mm, 5%) are accessory phases.

The sample from Sierra del Fraile is a quartz monzonite with porphyritic texture. The phenocrysts are mainly plagioclase (35% – 40%), K-feldspar (25% – 30%), quartz (25% – 30%) and biotite and/or hornblende (8% – 10%). The matrix is composed of quartz and feldspars. However, the sample presents intense hydrothermal alteration (*cf.* Martínez-Herrera, 1993). The biotite is altered to chlorite and the feldspars are altered to sericite.

U-Pb dating

Fifty-four analyses carried out on zircon grains from La Maroma intrusive (MAR), provided $^{206}Pb/^{238}Pb$ ages ranging from 36.9 ± 0.5 Ma to 228.0 ± 2.0 Ma. Thirty

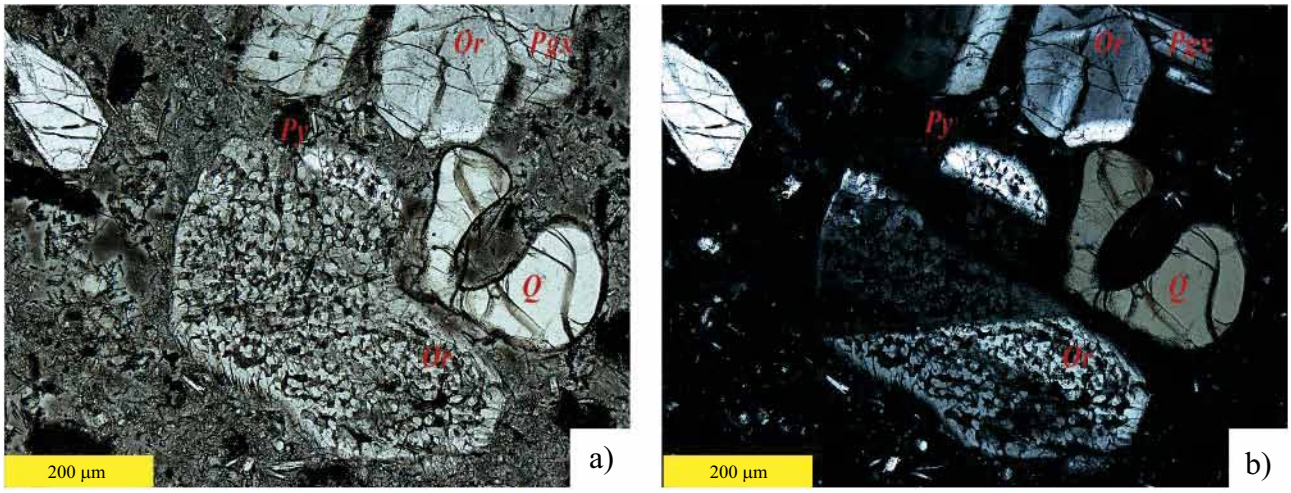

Figure 2. a) Microphotography of the Los Alamitos granodiorite (ARG sample) with plane polarized light; b) Same as "a" with crossed nicols. Note in both images the corroded quartz and the alteration of the orthoclase crystal (center part of image); Abbreviations used: *Plg*: plagioclase, *Ol*: olivine; *Idg*: Iddingsite; *Ol*: olivine; *Py*: pyrite; *Q*: quartz; *Or*: orthoclase.

analyses were discarded due to their high sigma errors (over 25%), or because of their $^{206}Pb/^{238}U$ and $^{207}Pb/^{235}U$ discordant ages. The remaining twenty-four $^{206}Pb/^{238}Pb$ ages range from 39.5 ± 0.2 Ma to 42.2 ± 0.3 Ma and form a tight cluster (Figures 3-4, and supplementary Table A1). These data yielded a weighted mean $^{206}Pb/^{238}U$ age of 40.8 ± 0.3 Ma (*n*=24; MSWD of 7.5), calculated using the Isoplot software (Ludwig, 2008). One subconcordant age of 228.0 ± 2.0 Ma, suggests inherited zircon cores of a Triassic magmatic event.

For the Real de Catorce intrusive (RCS, Figure 1) sixty-nine analyses provided $^{206}Pb/^{238}U$ ages dispersed between 34.6 ± 0.5 Ma and 2093.0 ± 86.0 Ma. Forty-nine analyses were discarded due to their high sigma errors, or their $^{206}Pb/^{238}U$ and $^{207}Pb/^{235}U$ discordant ages. The remaining twenty concordant ages range from 41.5 ± 0.2 Ma to 45.4 ± 0.3 Ma and form a tight cluster. The weighted mean crystallization age (Ludwig, 2008) of zircons from the Real de Catorce intrusive is 42.9 ± 0.5 Ma (*n*=21; MSWD of 20; Figure 3, Table A1).

Fifty-six analyses performed in zircon crystals separated from Los Alamitos intrusive (ARG, Figure 1) yielded $^{206}Pb/^{238}U$ ages in the range between 41.2 ± 0.2 Ma and 2521.0 ± 65.0 Ma. Twenty-six analyses were discarded for the same reasons as above. The remaining twenty concordant ages range from 41.9 ± 0.3 Ma to 49.0 ± 0.3 Ma and form a tight cluster. The weighted mean crystallization age (Ludwig, 2008) is 44.6 ± 0.8 Ma (*n*=25; MSWD of 38; Figure 3-4, Table A1). Thirteen zircon grains yielded concordant ages scattered between 49.0 ± 0.3 Ma and 1320.0 ± 19.0 Ma. They probably represent xenocrysts inherited from older country rocks, documenting assimilation. Particularly relevant to this group are the ages of *ca.* 160 Ma (*n*=2) correlative to the Bathonian age rhyolite flow that is found intercalated within the Middle Jurassic sedimentary formation (Barboza-Gudiño *et al.*, 2004). Other groups of concordant ages revealed the existence of four xenocrysts zircons including Ladinian (*ca.* 240 Ma, *n*=2), Silurian (*ca.* 420 Ma, *n*=1), Edicarian (*ca.* 620 Ma, *n*=1), and Stenian (*ca.* 1000 Ma, *n*=1) ages. Four discordant ages defining a discordia line with an upper intercept at 1100 Ma and a lower intercept at 54.4 ± 0.5 Ma, are in good agreement with inherited and crystallization ages, respectively.

For the Real de Catorce VMP-16 dyke sample (Figure 1), sixty-one analyses provide $^{206}Pb/^{238}U$ ages from 34.7 ± 0.3 Ma to 52.0 ± 2.0 Ma. Thirty-six analyses were discarded for the same reasons as above. The remaining twenty-five concordant ages range from 40.4 ± 0.3 Ma to 43.8 ± 0.4 Ma and form a tight cluster. The weighted mean crystallization age (Ludwig, 2008) is 41.8 ± 0.3 Ma (*n*=25; MSWD of 9; Figure 3, Table A1).

For the Real de Catorce VMS-34 dyke sample (Figure 1), forty analyses provide $^{206}Pb/^{238}U$ ages from 39.4 ± 0.3 Ma to 69.8 ± 0.4 Ma. Twelve analyses were discarded. The remaining twenty-eight concordant ages range from 40.9 ± 0.3 Ma to 44.0 ± 0.3 Ma and form a tight cluster. The weighted mean crystallization age (Ludwig, 2008) is 42.6 ± 0.3 Ma (*n*=28; MSWD of 8.3; Figure 3-4, Table A1).

Thirty-three analyses performed in El Fraile intrusive indicated $^{206}Pb/^{238}U$ ages ranging from 28.8 ± 0.4 Ma to 114.0 ± 1.0 Ma. Twenty analyses were discarded. The remaining thirteen concordant ages range from 34.2 ± 0.5 Ma to 36.6 ± 0.4 Ma and form a tight cluster. The weighted mean crystallization age (Ludwig, 2008) is 35.8 ± 0.4 Ma (*n*=13; MSWD of 4; Figure 3, Table A1).

Major and trace elements

The major and trace element contents of the intrusives (MAR, ARG, RCS, VMP-16 and VMS-34) are shown

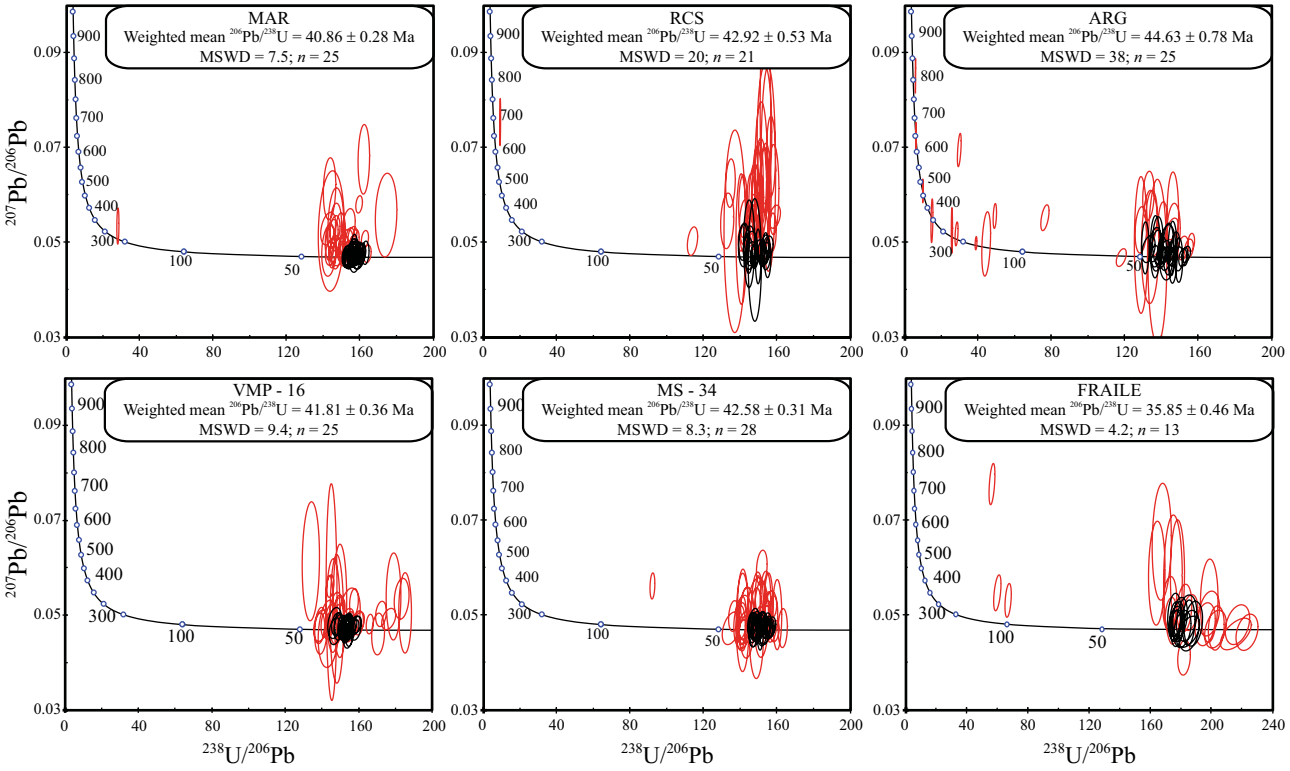

Figure 3. Concordia diagrams of the six samples dated by LA–ICPMS. Concordia, ages and errors are calculated using Isoplot 3.71 (Ludwig, 2008). Ellipses are 1-sigma errors. The ellipses in black correspond to the analysis used for the weighted mean age determination.

in Table 2. A regional geochemical dataset for El Fraile granodiorite (Pinto-Linares *et al.,* 2008) was considered here for comparison.

The major element contents (except K_2O) of all studied intrusive samples show no obvious correlation with increasing LOI, indicating that the original compositions of the samples have probably not been largely changed by alteration. In the TAS diagram (Figure 5) the samples plot in the granodiorite and quartz-monzonite fields. All these rocks show high-K calc-alkaline affinity (3.4 % < K_2O < 9.2 %; Figure 6); with a K_2O/Na_2O ratio ranging from 0.96 to 6.01. Within the A-B diagram (modified by Villaseca *et al.*, 1998),

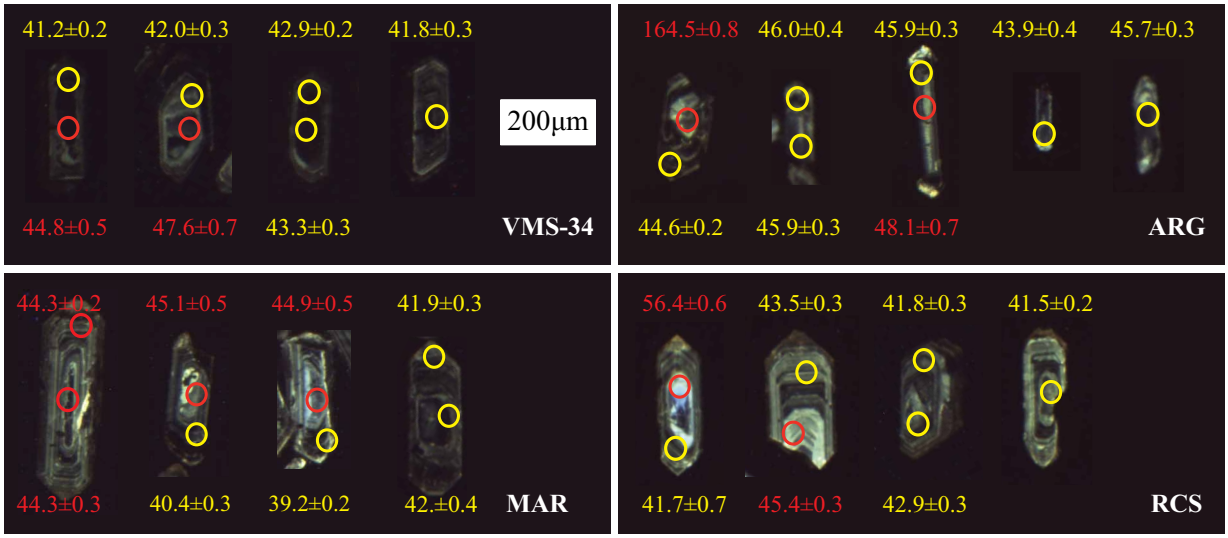

Figure 4. Cathodoluminescence images of the zircon dated. The white bar corresponds to a 200 µm scale. The spot is 34 µm in diameter. The reported ages are $^{206}Pb/^{238}U$ ages. Ages in yellow are used to calculate the sample age. The ages in red are from inherited zircon cores, not used in the calculated age.

Table 1. Major element oxides and trace elements analyzed for the chosen samples. * Total iron as Fe_2O_3; major element oxides in wt%, trace elements in ppm. See details on analysis procedures in the text.

Sample	**ARG**	**VMP-16 borehole**	**VMS-34 borehole**	**MAR**	**El Fraile**
Location	Rancho Los Alamaritos	Real de Catorce	Real de Catorce	La Maroma	La Paz
Rock	granodiorite	quartz monzonite	granodiorite	granodiorite	granodiorite
Lat. (ºN)	23.6094	23.6836	23.68312	23.5143	23.4115
Long. (ºW)	100.8584	100.8668	100.86922	100.8283	100.4254
Age (Ma)	44.6 ± 0.8	41.8 ± 0.4	42.5 ± 0.3	40.8 ± 0.3	36.8 ± 0.4
SiO_2 *(wt%)*	68.33	64.68	65.34	66.81	64.97
TiO_2	0.42	0.59	0.48	0.51	0.68
Al_2O_3	15.28	14.87	14.71	13.87	15.64
$Fe_2O_3^*$	2.52	3.26	3.00	3.15	3.45
MnO	0.04	0.22	0.07	0.05	0.04
MgO	1.52	1.90	1.78	1.66	1.06
CaO	2.60	1.85	2.99	2.40	4.82
Na_2O	3.49	0.13	0.97	2.39	2.80
K_2O	3.37	9.22	5.81	4.02	4.67
P_2O_5	0.15	0.16	0.15	0.16	0.25
LOI	2.54	2.99	5.09	3.73	-
Sum	100.25	99.86	100.36	98.75	98.38
Li *(ppm)*	33.8	31.4	38.3	47.2	-
Be	3.9	1.1	2.2	4.0	2.16
B	n.d.	n.d.	n.d.	n.d.	-
Sc	5.4	10.5	6.5	8.2	-
V	43.2	58.7	52.4	55.7	47.60
Cr	44.0	52.9	113.4	41.9	4.40
Co	4.9	7.5	9.5	7.9	4.76
Ni	17.5	16.8	83.6	24.9	-
Cu	9.1	21.1	14.8	25.7	135.74
Zn	45.6	122.6	193.5	143.0	82.50
Ga	20.1	17.1	16.9	19.2	21.91
Rb	135.1	314.8	197.3	162.5	167.14
Sr	607.6	348.1	220.1	204.4	512.97
Y	16.2	18.8	16.5	51.0	16.57
Zr	152.3	211.5	141.3	119.0	191.93
Nb	11.0	12.1	10.7	12.5	10.43
Mo	2.0	1.7	11.1	2.0	14.36
Sn	3.0	3.0	4.1	3.8	10.66
Ba	966.0	6683.6	846.0	687.3	752.14
Pb	32.0	11.3	36.8	25.5	12.80
Th	11.1	13.4	11.1	12.7	10.39
U	5.4	4.3	4.8	5.7	3.54
Hf	4.1	5.4	3.8	3.3	5.13
Ta	1.1	1.1	1.2	1.4	1.10
W	1.7	1.7	2.8	2.2	4.10
Tl	2.8	7.2	3.5	2.0	-
La	32.5	33.7	25.2	57.9	29.50
Ce	58.1	66.2	49.9	120.6	65.17
Pr	7.5	8.0	6.1	16.7	8.12
Nd	26.8	29.1	22.4	65.2	32.27
Sm	4.9	5.6	4.4	13.5	6.46
Eu	1.2	1.9	1.0	2.6	1.54
Gd	3.9	4.6	3.8	12.4	5.20
Tb	0.6	0.7	0.6	1.7	0.66
Dy	3.0	3.5	3.0	8.7	3.61
Ho	0.6	0.7	0.6	1.5	0.55
Er	1.5	1.8	1.5	3.7	1.70
Yb	1.4	1.7	1.5	2.7	1.53
Lu	0.2	0.2	0.2	0.4	0.23
Sb	3.0	10.0	25.3	3.2	8.25
Cs	33.8	7.7	8.2	6.4	8.27

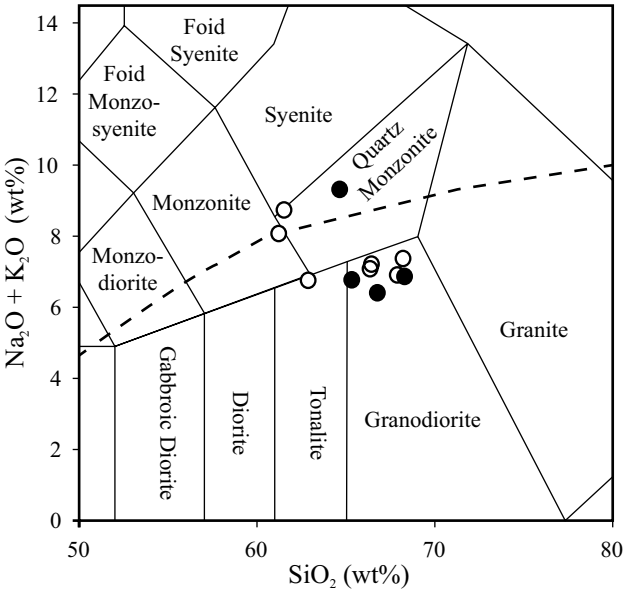

Figure 5. Total Alkali *vs.* Silica (TAS) diagram (after Middlemost, 1997) of the Sierra de Catorce samples (black dots) in comparison with those of the Sierra del Fraile (open dots) reported by Pinto-Linares *et al.* (2008).

the Sierra de Catorce samples plot on the moderately peraluminous field with A [= Al-(K+Na+2Ca)] values from 22.6 to 27.6, (Figure 7). None of the analysed rocks in this study contain normative corundum; they present ASI values [molar $Al_2O_3/(CaO+Na_2O+K_2O)$] less or equal than 1.1. Thus, these rocks are classified as I-type granitoids, that plot close to the limit with the S-type (Chappell and White, 2001). The Fraile quartzmonzonite present lower ASI values (0.73 to 0.97), and is clearly an I-type granitoid. According to their relative low Fe* [= $FeO_{total}/(FeO_{total}+MgO)$] values, all the Sierra de Catorce intrusive bodies and several samples of Fraile are magnesian granitoids (Figure 8, Frost *et al.*, 2001); they plot inside the field of cordilleran granites, which are considered as I-type granites (Chappell and White, 1974) and equivalent to the volcanic arc granites of Pearce *et al.* (1984), or island arc and continental arc granitoids of Maniar and Piccoli (1989) (see Frost *et al.,* 2001).

Chondrite-normalized (Sun and McDonough, 1989) rare earth element (REE) patterns illustrate that all the samples are similar and display a strong fractionation from light REE to middle REE ($11.3< (La/Yb)_N <15.5$), a general absence of a significant Eu anomaly and a slight fractionation from MREE to HREE ($2.0< (Gd/Yb)_N <3.7$) with a concave-upward shape (Figure 9a). Such REE pattern is consistent with the existence of two different magma sources or the interaction of two differentiation processes (Rollinson, 1993). The presence of inherited zircons indicates assimilation of country rocks. On the other hand, magma mixing is common in cordilleran granites (Brown, 1977). If there were only a single magma source from which the granitoids differentiated by fractional crystallization, a pronounced negative Eu anomaly and a stronger fractionation from LREE to HREE would be expected.

Primitive mantle-normalized incompatible element spider diagrams reveal similar trends for all the SDCR and Fraile rocks with obvious negative anomalies in Nb, P and Ti (Figure 9b) and positive anomalies in Pb, which reflect a subduction-related signature (Pearce *et al.*, 1984, 1990). All

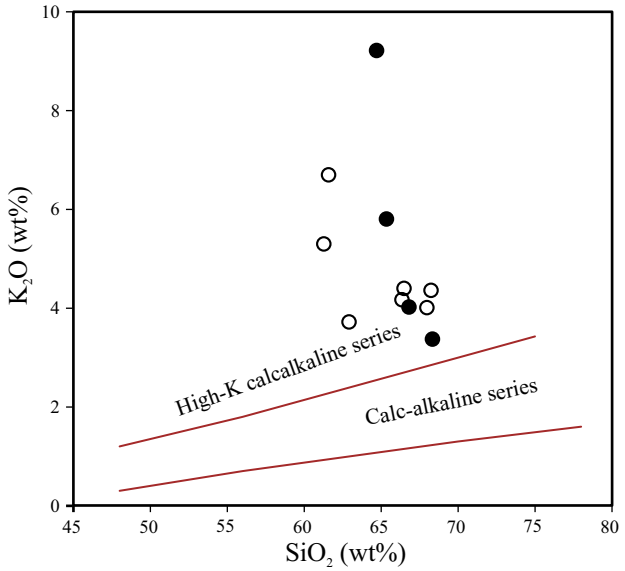

Figure 6. K_2O *vs.* SiO_2 variation diagram of igneous rocks from the studied area. Boundaries from Peccerillo and Taylor (1976). Black dots: Sierra de Catorce samples; Open dots: Sierra El Fraile samples from Pinto-Linares *et al.* (2008).

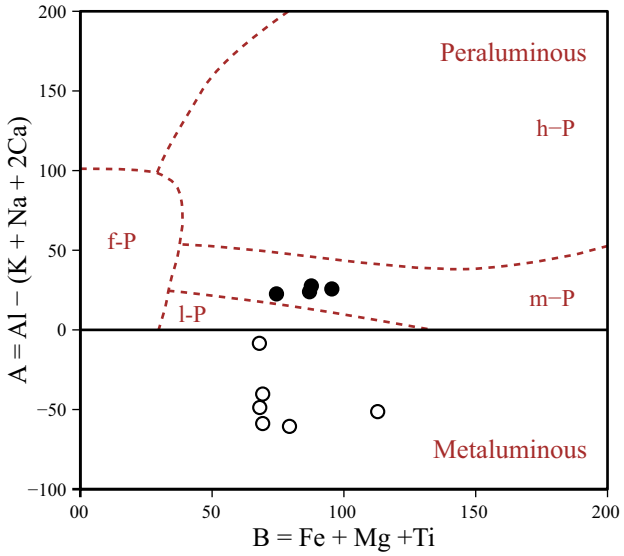

Figure 7. A-B plot (modified by Villaseca *et al.*, 1998), with A=[Al-(K+Na+2Ca)] and B=Fe+Mg+Ti (gram-atoms×10^3 of each element in 100 g of materia). Note that all the Sierra de Catorce samples (black dots) are moderately peraluminous, while the Sierra El Fraile samples (open dots) from Pinto-Linares *et al.* (2008) are metaluminous. f-P: highly felsic peraluminous: l-P: low peraluminous; m-P: moderately peraluminous; h-P: highly peraluminous.

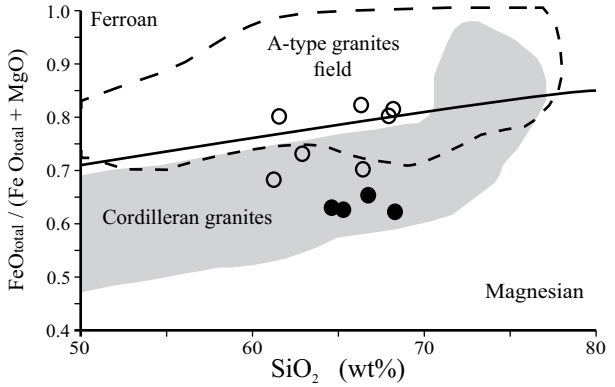

Figure 8. SiO_2 *vs.* $FeO_{tot}/(FeO_{tot}+MgO)$ diagram (after Frost *et al*., 2001). Black dots: Sierra de Catorce samples; open dots: Sierra El Fraile samples from Pinto-Linares *et al.* (2008).

the samples are considerably enriched in light incompatible lithophile elements (LILE) (in the order of 100–1000 times over the reference values) and in light rare earth elements (LREE) (in the order of a few 10 to a few 100), but only slightly enriched in high field strenght elements (HFSE), except Nb, (in the order of 10–100) and with very low HREE contents. The relative enrichment in Th, Rb and U may also have resulted from assimilation combined with fractional crystallization processes (Wilson, 1989; Rollinson, 1993). The high concentrations of Ba (466 to 6683 ppm) and Sr (204 to 607 ppm) (Table 1) are in the range of values observed in classical continental arc granites (Qian *et al.*, 2003), and more precisely as high-Ba-Sr granitoids (Tarney and Jones, 1994).

Geotectonically, the SDCR intrusives are classified as volcanic arc granites in the limit with the syn-collisional granite field (Figure 10a and 10b; Pearce *et al.*, 1984). Relatively low Rb/Zr ratios and Nb concentrations (Figure 11) further indicate a normal, calc-alkaline continental arc setting for the studied granitoids (Brown, 1984).

DISCUSSION

As a whole, the distribution of the intrusion ages (Figure 3) allows distinguishing two separate Eocene magmatic events in the SDCR. The granitoids of Sierra de Catorce define a middle Eocene magmatic pulse, while El Fraile intrusive has a late Eocene age.

The age distribution may reflect a cluster of discrete magmatic pulses associated with Los Alamitos (AGS: 44.6 ± 0.8 Ma) and La Maroma (MAR: 40.9 ± 0.3 Ma) stocks (Figure 3, Table A1). The lack of deformation indicates post-orogenic emplacement, in agreement with the pre-middle Eocene chronology proposed by Cuéllar-Cárdenas *et al.,* (2012) for the Laramide orogeny in this area.

The Lutetian age of the Sierra de Catorce intrusives (*ca.* 42 Ma) indicates that igneous activity was contemporaneous with the Zimapan Cu-Zn skarn deposit (Hidalgo state; 41 ± 1 to 44 ± 1 Ma, K-Ar in whole rock; Vassallo *et al.*, 2008), the Zn-Cu skarn at Charcas (San Luis Potosí state, 43 ± 3 Ma, K-Ar in orthoclase; Mújica-Mondragón and Jacobo-Albarrán, 1983) and Concepción del Oro district (*ca.* 32 to 45 Ma, U-Pb in zircon; González-Guzmán, 2012). As a whole, this set of intrusions represents the first magmatic and mineralizing episodes related to the post Laramide volcanic activity in the region. It may also correlate with the uppermost part of the Lower Volcanic Complex of the Sierra Madre Occidental volcanic province (McDowell and Clabaugh, 1979; Ferrari *et al.*, 2007).

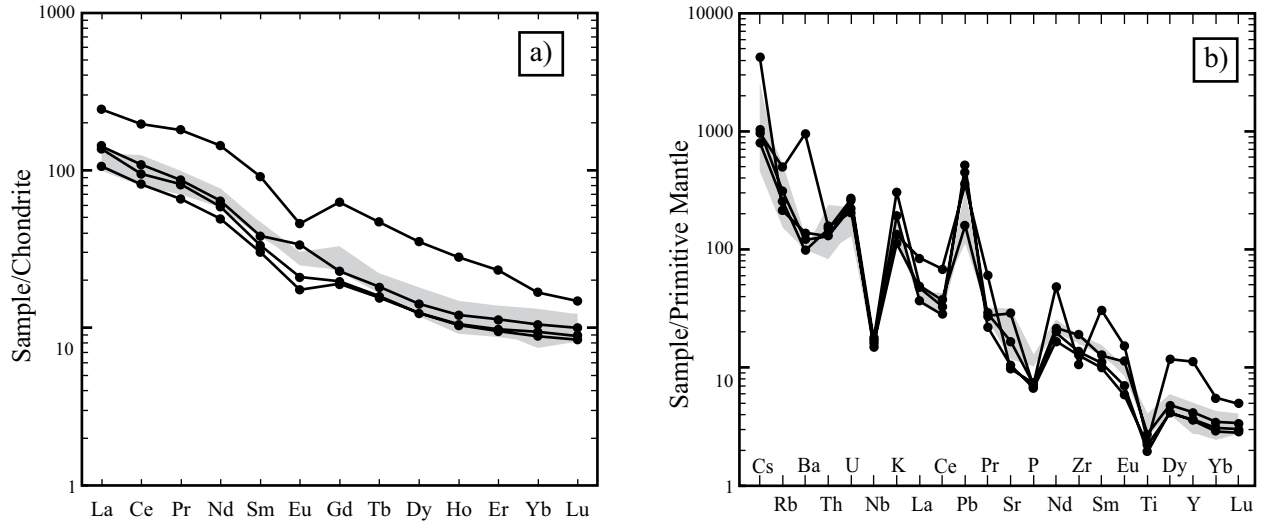

Figure 9. a) Chondrite-normalized (Sun and McDonough, 1989) REE patterns and (b) multi-element plots for Real de Catorce granitoids normalized to primitive mantle (Sun and McDonough, 1989). In both diagrams the shaded area represents the composition of the Sierra del Fraile granitoids (Pinto-Linares *et al.*, 2008).

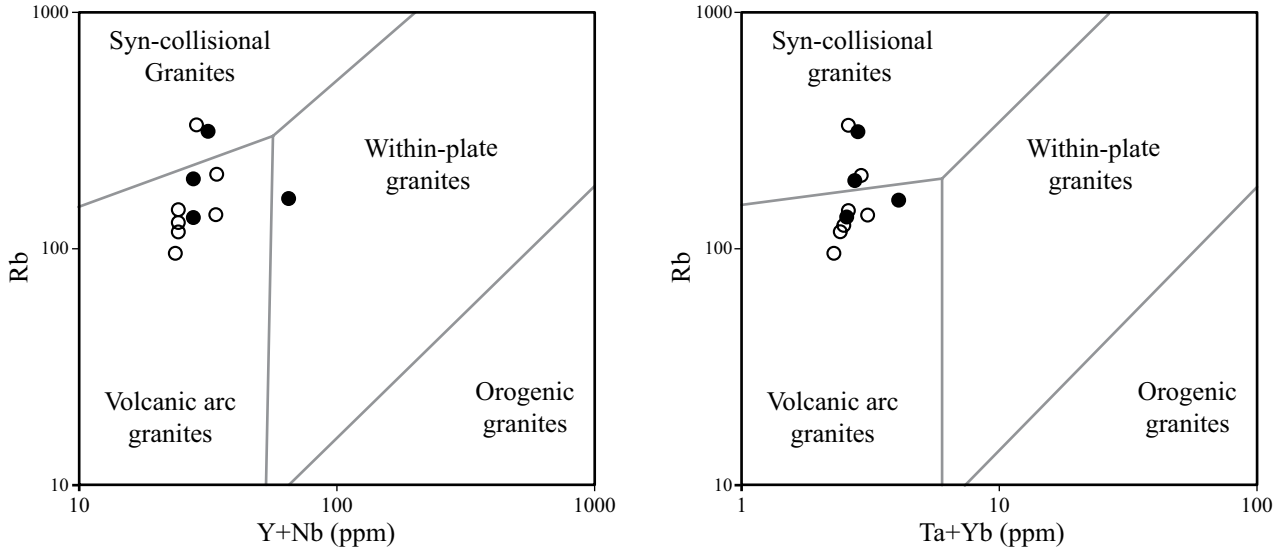

Figure 10. Tectonic discriminant diagrams (Pearce *et al.*, 1984) for the studied intrusive. Both Sierra de Catorce and the Sierra del Fraile samples plot in the field of volcanic arc granites, in the limit with the field of syn-collisional granites. Black dots: Sierra de Catorce samples; Open dots: Sierra del Fraile samples from Pinto-Linares *et al.* (2008).

Magma origin

The petrography of granitoids shows a porphyric texture. The granitoids have the same mineralogical composition and porphyric minerals ratios. The SDCR granitoids are metaluminus to weakly peraluminus, consistent with the presence of amphibole, as well as the absence of muscovite.

The whole-rock geochemical signatures indicate that the middle to late Eocene intrusives correspond to continental arc magmatism (I-type granitoids). I-type granites can be formed in a variety of ways. They are the result of a multi-source/multi-stage phenomenon.

Discrimination diagrams (Figure 10 and 11) indicate that the SDCR were generated in a mature continental arc environment. But, in contrast to what is observed in typical I-type granitoids, the intrusive rocks of the SDCR present a high concentration of Ba and Sr, and high Sr/Y and La/Yb ratio values. These characteristics are comparable to those reported for high Ba-Sr granitoids originated by partial melting of an enriched lithospheric mantle in post-orogenic environments, followed by assimilation of continental crust (Tarney and Jones, 1994). This model is congruent with the local geodynamical evolution. Humpreys *et al.,* (2003) and, more recently, Cuéllar-Cárdenas *et al.* (2012), propose a migration to the East for the Laramide orogeny. Following Cuéllar-Cárdenas *et al.* (2012), the deformation peak in the SDCR area occurs at *ca.* 60 Ma.

Because Zr/Hf decreases with increasing evolution of a silicate melt, some authors have proposed this ratio as a fractionation index for granitic rocks (Bea *et al.*, 2006; Zaraysky *et al.*, 2007). The SDCR show Zr/Hf ratios characteristic of non-evolved granites, (Zr/Hf = 36–39). As well, the relation between the SiO_2 and REE concentration does not indicated fractional crystallization as a main process.

We conclude that the formation of SDCR granitoids is related to multiple sources and have a complex history. The Ba-enrichment trend in the SDCR granitoids is interpreted as the evidence of slab dehydration and generation of LILE-enriched fluids that produced partial melting of the mantle wedge just below the base of a thick and light continental crust. During their ascent these melts underwent fractional crystallization, as well as assimilation and melting of crustal components (Hildreth and Moorbath, 1988).

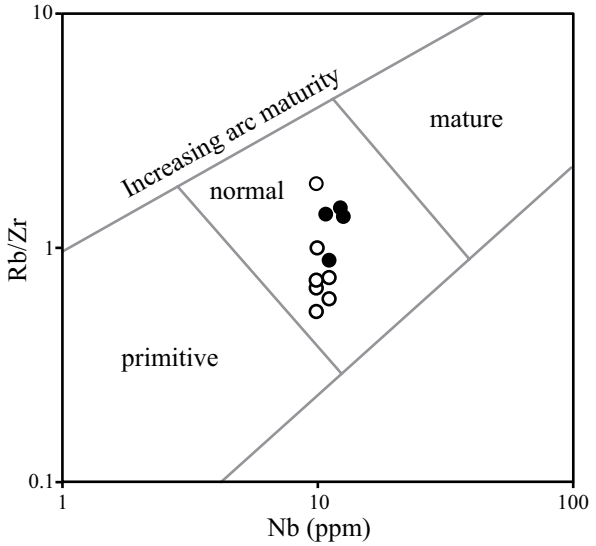

Figure 11. Nb *vs.* Rb/Zr bivariate plot with fields after Brown (1984), indicating the maturity grade of the volcanic arcs. Both Sierra de Catorce and the Sierra del Fraile samples plot in the field of normal continental arcs. Black dots: Sierra de Catorce samples; Open dots: Sierra del Fraile samples from Pinto-Linares *et al.* (2008).

CONCLUSIONS

The Sierra de Catorce and the El Fraile samples correspond to a N-S dyke and elongate stock that consist predominantly of monzogranites and granodiorites. They represent two distinctive magmatic pulses at 45 and 38 Ma, respectively. Inherited zircon grains, which were incorporated into the granodioritic magma during its formation and/or ascent through the crust highlight the presence of a Mesoproterozoic lower crust beneath the Mesa Central.

Major and trace element compositions and comparison with similar rocks in Andean Cordillera suggest that the arc granitoids were emplaced in a thick continental crust. The origin of the granitoids in this locality can be explained from a complex model that involves partial melting of metasomatized mantle in a post-orogenic scenario. During its ascent and emplacement, the magmas underwent a process of fractional crystallization coupled with assimilation of crustal material.

ACKNOWLEDGEMENTS

Our deep thanks to Ing. Ramón Dávila, Chief Operating Officer of First Majestic and Lic. José Cerrillo Chowell, General Director of Negociación Minera Santa María de La Paz y Anexas, S.A. de C.V. for their support and permission to publish. Special thanks to Porfirio Pinto-Linares and Jorge Aranda, for help in fieldwork in the Sierra de Catorce and to Carlos Ortega Obregón and Ofelia Pérez Arvizu for assitence at CGEO laboratory. We sincerely thank Dr. García-Casco, Dr. Barboza-Gudiño, Dr. Solari, Dr. Alaniz-Álvarez and Dr. Luca Ferrari for their constructive reviews. This study was financially supported by UNAM-PAPIIT project IN100707, IN109410-3, and CONACyT project 81584.

APPENDIX A. SUPPLEMENTARY DATA

Table A1 can be found at the journal web site <http://rmcg.unam.mx/>, in the table of contents of this issue.

REFERENCES

Alaniz-Álvarez, S.A., Nieto-Samaniego, A.F., 2005, El sistema de fallas Taxco-San Miguel de Allende y la Faja Volcánica Transmexicana, dos fronteras tectónicas del centro de México activas durante el Cenozoico: Boletín de la Sociedad Geológica Mexicana, 57(1), 65-82.

Aranda-Gómez, J.J., Luhr, J.F., 1996, Origin of the Joya Honda maar, San Luis Potosí, México: Journal of Volcanology and Geothermal Research, 74, 1-18.

Barboza-Gudiño, J.R., Álvarez-Maya, V.M., Torres-Hernández, J., 1998, Informe de la Carta Geológico Minera y Geoquímica; Hoja Real de Catorce; Escala 1:50.000, technical report, Consejo de Recursos Minerales, 258 p.

Barboza-Gudiño, J.R., Hoppe, M., Gómez-Anguiano, M., Martínez-Macías, P.R., 2004, Aportaciones para la interpretación estratigráfica y estructural de la porción noroccidental de la Sierra de Catorce, San Luis Potosí, México: Revista Mexicana de Ciencias Geológicas, 21(2), 299-319.

Barboza-Gudiño, J.R., Orozco-Esquivel, M.T., Gómez-Anguiano, M., Zavala-Monsiváis, A., 2008, The Early Mesozoic volcanic arc of western North America in northeastern Mexico: Journal of South American Earth Sciences, 25, 49-63.

Barboza-Gudiño, J.R., Molina-Garza, R.S., Lawton, T.F., 2012, Sierra de Catorce: Remnants of the ancient western equatorial margin of Pangea in central Mexico, *in* Aranda-Gómez, J.J., Tolson, G., Molina-Garza, R.S. (eds.), The Southern Cordillera and Beyond: GSA Field Guides, 25, 1-18

Bea, F., Montero, P., Ortega, M., 2006, A LA-ICPMS evaluation of Zr reservoirs in common crustal rocks: implications for a Zr and Hf geochemistry, and zircon-forming processes: Canadian Mineralogist, 44, 693-714.

Blauser, W.H., 1979, Geology of the Southern Sierra de Catorce and Stratigraphy of the Taraises Formation in North-Central Mexico: The Univerity of Texas at Arlington, Master Thesis, 91 p.

Brown, C.G., 1977, Mantle origin of Cordilleran granites: Nature, 265, 21 - 24.

Brown, M., 1984, The generation, segregation, ascent and emplacement of granite magma: the migmatite to crustally derived granite connection in thickened orogens: Earth-Science Reviews, 36, 83-130.

Carrillo-Bravo, J., 1968, Reconocimiento geológico preliminar de la porción central del Altiplano Mexicano: Petróleos Mexicanos, Technical Report, 89 p.

Carrizales-Ibarra, M., 1989, Estudio geo-económico del área central, minas de San José, Tierras Negras, Municipio. de Catorce, S.L.P.: Mexico, Universidad Autónoma de San Luis Potosí, Escuela de Ingeniería, tesis de licenciatura, 42 p.

Chappell, B.W., White, J.R., 1974, Two contrasting granite types: Pacific Geology, 8, 173-174.

Chappell, B.W., White, J.R., 2001, Two contrasting granite types: 25 years later: Australian Journal of Earth Sciences, 48, 489-499.

Chippendale, A., 1910, Matehuala district; supplementary report on the silver Mines of Maroma: Servicio Geologico Mexicano, unpublished report, 152 p.

Cuéllar-Cárdenas, M.A., Nieto-Samaniego, A.F., Levresse, L., Alaniz-Álvarez, S.A., Ortega-Obregón, C., López-Martínez, M., Solari, L., 2012, Limites temporales de la deformación contractiva Laramide en el centro de México: Revista de Ciencias Geologicas Mexicanas, 29(1), 179-203.

Demant, A., 1978, Características del Eje Neovolcánico Transrnexicano y sus problemas de interpretación: Universidad Nacional Autónoma de México, Instituto de Geología, Revista, 2, 172-187.

Ferrari, L., Valencia-Moreno, M., Bryan, S., 2007, Magmatism and tectonics of the Sierra Madre Occidental and its relation with the evolution of the western margin of North America, *in* Alaniz-Álvarez, S.A., Nieto-Samaniego, Á.F. (eds.), Geology of México: Celebrating the Centenary of the Geological Society of México: Geological Society of America Special Paper 422, 1-39.

Frost, B.R., Barnes, C.G., Collins, W.J., Arculus, R.J., Ellis, D.J., Frost, C.D., 2001, A Geochemical Classification for Granitic Rocks: Journal of Petrology, 42, 2033-2048.

Geoffrey I.R., 1979, Geology of the Northernmost Sierra de Catorce and Stratigraphy and Biostratigraphy of the Cuesta del Cura Formation in Northeastern and Northcentral Mexico: The University of Texas at Arlingon, Master Thesis, 176 p.

González-Guzmán, R., 2012, Origen y Evolución Magmática del Cinturón de Intrusivos de Concepción del Oro: Universidad Autónoma de Nuevo León, Facultad de Ciencias de la Tierra, M. Sc. Thesis, 205 p.

Gunnesch, K.A., Torres-del Angel, C., Cuba-Castro, C., Saenz, J., 1994, The Cu-Au Skarn and Ag-Pb-Zn vein deposits of La Paz, northeastern Mexico: Mineralogical, paragenetic and fluid inclusion characteristics: Economic Geology, 98, 455-489.

Hildreth,W., Moorbath, S.,1988, Crustal contributions to arc magmatism in the Andes of Central Chile: Contributions to Mineralogy and Petrology, 98, 455-489.

Hoppe, M., 2000, Geologische Kartierung (1:10,000) im Gebiet Ojo de Agua, nordwestliche Sierra de Catorce und sedimentpetrologische Untersuchungen an prä.oberjurassischen Sedimenten ("Zacatecas formation"): Technische Universität Clausthal, Master thesis, 182 p.

Lozano, R., Bernal, J.P., 2005, Characterization of a new set of eight geochemical reference materials for XRF major and trace element analysis: Revista Mexicana de Ciencias Geológicas, 22(3), 329-344.

Ludwig, K.L., 2008, Isoplot 3.7. A geochronological toolkit for Microsoft Excel: Berkeley Geochronology Center Special Publication, 4, 1-77.

Luhr, J.F., Aranda-Gómez, J.J., 1997, Mexican peridotite xenoliths and tectonic terranes: correlations among vent, location, texture, temperature, pressure, and oxygen fugacity: Journal of Petrology, 38, 1075-1112.

Maniar, P.D., Piccoli, P.M., 1989, Tectonic discrimination of granitoids: Geological Society of America Bulletin, 101, 635-643.

Martínez-Herrera, N., 1993, Cartografía Geológica, estudio petrográfico y mineralógico de los yacimientos polimetálicos (Cu-Pb-Zn-Ag) del distrito La Paz, S.L.P.: México, Universidad Autónoma de Nuevo León. Tesis de Licenciatura, 85 p.

Martínez-Macías, P.R., 2004, Litoestratigrafía de la Sierra de Catorce; San Luís Potosí, México, Universidad Nacional Autónoma de México, Posgrado en Ciencias de la Tierra, tesis de Maestría, 175 p.

McDowell, F.W., Clabaugh, S.E., 1979, Ignimbrites of the Sierra Madre Occidental and their relation to the tectonic history of western Mexico, *in* Chapin, C.E., Elston, W.E. (eds.), Ash-Flow Tuffs: Geological Society of America Special Paper 180, 113-124.

Middlemost, E.A.K., 1997, Magmas, Rocks and Planetary Development: Longman, Harlow, 299 p.

Mori, L., Gómez-Tuena, A., Cai, Y., Goldstein, S.L., 2007, Effects of prolonged flat subduction on the Miocene magmatic record of central Trans Mexican Volcanic Belt: Chemical Geology, 244, 452-473.

Mújica-Mondragón, R., Jacobo-Albarrán, J., 1983, Estudio petrogenético de las rocas ígneas y metamórficas del Altiplano Mexicano: Instituto Mexicano del Petróleo, Subdirección Técnica de Exploración, Proyecto C–1156, technical report, 87 p.

Nieto-Samaniego, A.F., Alaniz-Álvarez, S.A., Camprubí, A., 2005, La Mesa Central de México: estratigrafía, estructura y evolución tectónica cenozoica: Boletín de la Sociedad Geológica Mexicana, 57, 285-318.

Olóriz, F., Villaseñor, A.B., González-Arreola, C., Westermann, G.E.G., 1999, Ammonite biostratigraphy and correlations in the Upper Jurassic-Lowermost Cretaceous La Caja Formation of northcentral Mexico (Sierra de Catorce, San Luis Potosí), *in* Olóriz, F., Rodríguez-Tovar, F.J. (eds.), Advancing research on living and fossils cephalopods: New York, Kluwer Academic - Plenum Publishers, 463-492.

Orozco-Esquivel, M., Nieto-Samaniego, A., Alaniz-Álvarez, S.A., 2002, Origin of rhyolitic lavas in the Mesa Central, Mexico, by crustal melting related to extension: Journal of Volcanology and Geothermal Research, 118, 37-56.

Pearce, J.A., Harris, N.B.W., Tindle, A.G., 1984, Trace element discrimination diagrams for the tectonic interpretation of granitic rocks: Journal of Petrology, 25, 956-983.

Pearce, J.A., Bender, J.F., De Long, S.E., Kidd, W.S.F., Low, P.J., Güner, Y., Şaroğlu, F., Yılmaz, Y., Moorbath, S., Mitchell, J.G., 1990, Genesis of collision volcanism in Eastern Anatolia, Turkey: Journal of Volcanology and Geothermal Research, 44, 189-229.

Peccerillo, R., Taylor, S.R., 1976, Geochemistry of Eocene calcalkaline volcanic rocks from the Kastamonu area, northern Turkey: Contributions to Mineral Petrology, 58, 63-81.

Pinto-Linares, P. J., Levresse, G., Tritlla, J., Valencia, V., Torres-Aguilera, M., J., González, M., Estrada, D., 2008, Transitional adakite-like to calc-alkaline magmas in a continental extensional setting at La Paz Au-Cu skarn deposits, Mesa Central, Mexico: metallogenic implications: Revista Mexicana de Ciencias Geológicas, 25, 39-58.

Qian, Q., Chung, S.L., Lee, T.Y., Wen, D.J., 2003, Mesozoic high-Ba-Sr granitoids from North China: geochemical characteristics and geological implications: Terra Nova, 15, 272-278.

Rollinson, H.R., 1993, Using geochemical data: evaluation, presentation, interpretation: New York, Longman Scientific and Technical, 384 p.

Solari, L.A., Gómez-Tuena, A., Bernal, J.P., Pérez-Arvizu, O., Tanner, M., 2010, U-Pb zircon geochronology by an integrated LA-ICPMS microanalytical workstation: achievements in precision and accuracy: Geostandards and Geoanalytical Research, 34(1), 5-18.

Sun, S.S., McDonough, W.F., 1989, Chemical and isotopic systematics of oceanic basalts: implications for mantle composition and processes, *in* Saunders, A.D., Norry, M.J. (eds.), Magmatism in the Ocean Basins: Geological Society of London,Special Publication 42, 313-345

Tarney, J., Jones, C.E., 1994, Trace element geochemistry of orogenic igneous rocks and crustal growth models: Journal of Geological Society London, 151, 855-868.

Tuta, Z.H., Sutter, J.F., Kesler, S.E., Ruiz, J., 1988, Geochronology of mercury, tin, and fluorine mineralization in Northern Mexico: Economic Geology, 83, 1931-1942.

Vassallo, L., Solorio, J.G., Ortega-Rivera, M.A., Sousa, J.E., Olalde, G., 2008, Paleogene magmatism and associated skarn-hydrothermal mineralization in the central part of Mexico: Bol-e, 4, 3, <http://www.geociencias.unam.mx/~bole/eboletin/aVassallo0908.pdf>.

Villaseca, C., Barbero, L., Herreros, V., 1998, A re-examination of the typology of peraluminous granite-types in intracontinental orogenic belts: Transactions of the Royal Society of Edinburgh: Earth Sciences, 89, 113-119.

White, D.E., Gonzáles, R.J., 1946, San José antimony mines near Wadley, State of San Luis Postosí, México: United States Geological Survey, Geological Investigations in the American Republics, Bulletin 946-E, 131-153.

Wilson, M., 1989, Igneous petrogenesis, A global tectonic approach: London, Unwin Hyman, 466 p.

Zárate del Valle, P.F., 1982, Geología y análisis metalogénico de la Sierra de Catorce: Boletín de la Sociedad Geológica Mexicana, 43, 1-21.

Zaraysky, G.P., Alfereva, J.O., Udoratina, O.V., 2007, Geochemical features of the Etyka tantalum deposit in Eastern Transbaikalia, *in* Sixth International Hutton Symposium, Stellenbosch University, South Africa, 232-233.

Manuscript received: December 16, 2012
Corrected manuscript received: February 2, 2013
Manuscript accepted: February 20, 2013